Forecasting the New York City Urban Heat Island and Sea Breeze during Extreme Heat Events

TALMOR MEIR, PHILIP M. ORTON, AND JULIE PULLEN

Stevens Institute of Technology, Hoboken, New Jersey

TEDDY HOLT AND WILLIAM T. THOMPSON

Marine Meteorology Division, Naval Research Laboratory, Monterey, California

MARK F. AREND

CUNY CREST Institute, City College of the City University of New York, New York, New York

(Manuscript received 17 December 2012, in final form 26 July 2013)

ABSTRACT

Two extreme heat events impacting the New York City (NYC), New York, metropolitan region during 7–10 June and 21–24 July 2011 are examined in detail using a combination of models and observations. The U.S. Navy's Coupled Ocean–Atmosphere Mesoscale Prediction System (COAMPS) produces real-time forecasts across the region on a 1-km resolution grid and employs an urban canopy parameterization to account for the influence of the city on the atmosphere. Forecasts from the National Weather Service's 12-km resolution North American Mesoscale (NAM) implementation of the Weather Research and Forecasting (WRF) model are also examined. The accuracy of the forecasts is evaluated using a land- and coastline-based observation network. Observed temperatures reached 39°C or more at central urban sites over several days and remained high overnight due to urban heat island (UHI) effects, with a typical nighttime urban–rural temperature difference of 4°–5°C. Examining model performance broadly over both heat events and 27 sites, COAMPS has temperature RMS errors averaging 1.9°C, while NAM has RMSEs of 2.5°C. COAMPS high-resolution wind and temperature predictions captured key features of the observations. For example, during the early summer June heat event, the Long Island south shore coastline experienced a more pronounced sea breeze than was observed for the July heat wave.

1. Introduction

Increasing computational resources and the continual improvement of parameterizations within atmospheric models have enabled high-resolution atmospheric forecasting at small scales. The importance of resolution for accurately reproducing mesoscale structures has long been recognized, and model resolutions have been reduced from hundreds of kilometers in the mid-1950s (Mass et al. 2002) to only a few meters in recent years (Loughner et al. 2011; Cohan et al. 2006; Jimenez et al. 2006). Although urban weather is often driven by large synoptic and mesoscale features, weather patterns unique to urban environments arise from the local characteristics of the urban setting: large areas covered by buildings, paved streets, reduced evapotranspiration due to lack of vegetation, and generation of waste heat (National Academy of Sciences 2012). To better prepare and respond to growing urban populations, the field of urban meteorology has grown to predict a wide set of environmental parameters at relatively fine temporal and spatial scales (National Research Council 2012). Recent studies have shown that high-resolution simulations can be more accurate in simulating mesoscale features and localized variability (Loughner et al. 2011; Cohan et al. 2006; Jimenez et al. 2006). The work reported here aims to map at fine resolution the pattern of extreme urban temperatures during two recent heat waves in the New York City (NYC), New York, metropolitan region.

New York City has an area of 790 km^2, a population of 8 million, and contains five boroughs that are all

Corresponding author address: Talmor Meir, Stevens Institute of Technology, Ocean Engineering, Castle Point on Hudson, Hoboken, NJ 07030-5991.
E-mail: tmeir@stevens.edu

DOI: 10.1175/WAF-D-13-00012.1

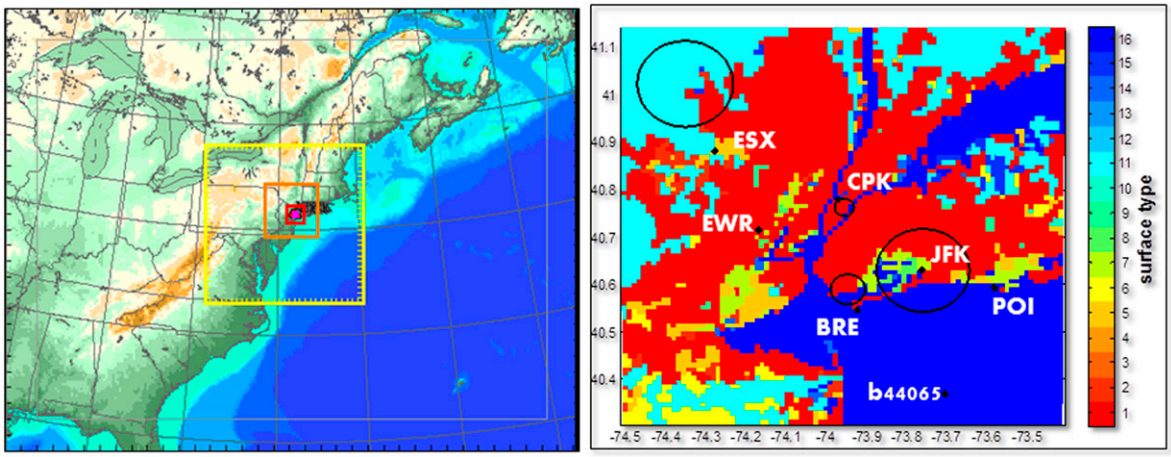

FIG. 1. (left) COAMPS nested grids and (right) the 1-km-resolution grid area of NYC, with stations and NDBC ocean buoy (b44065). COAMPS nests are 1 (36 km), 2 (12 km), 3 (4 km), 4 (1 km), and 5 (0.333 km). COAMPS grid-4 vegetation type derived from the following 1-km USGS land-use categories: 1, urban and built-up land; 2, dryland cropland and pasture; 3, irrigated cropland and pasture; 4, mixed dryland–irrigated cropland and pasture; 5, cropland–grassland mosaic; 6, cropland–woodland mosaic; 7, grassland; 8, shrubland; 9, mixed shrubland–grassland; 10, savanna; 11, deciduous broadleaf forest; 12, deciduous needle leaf forest; 13, evergreen broadleaf forest; 14, evergreen needle leaf forest; 15, mixed forest; and 16, water bodies.

influenced by the marine coastal atmosphere. NYC lies at the center of a broader urban and suburban metropolitan region, with Long Island extending to the east and New Jersey and the city of Newark to the west and southwest. Both NJ and Long Island are bordered by the coastal waters of the Atlantic (Fig. 1). NYC and its surrounding urbanized region generate a pronounced urban heat island (UHI) effect, whereby the urban region acts as a nocturnal heat reservoir relative to the surrounding rural environments (e.g., Bornstein 1968).

Rosenzweig et al. (2009) found the UHI effect to be of particular public policy concern during the summer, because elevated surface air temperatures are associated with an increase in electricity demand for air conditioning, air pollution, and heat-stress-related mortality (see also Rosenfeld et al. 1995; Sailor 2011). During a heat wave the atmospheric conditions are usually characterized by low wind speeds and higher temperatures (Rosenzweig et al. 2009), thus permitting urban temperatures to remain elevated for longer periods and possibly extend farther out into the rural surroundings. As a result, during a heat wave the city does not typically receive cool nocturnal temperatures to provide local relief. Tan et al. (2009) documented that the longest-lasting heat waves occur in urban areas, showing that the elevated warming and duration of urban heat waves is caused almost entirely by the UHI effect. Gedzelman et al. (2003) examined the climatology of the UHI for NYC and found that in all seasons the UHI ramps up rapidly in late afternoon, is maximal from midnight through the early morning, and shuts down even more rapidly after dawn. NYC's UHI was found to have an average magnitude of 3°C in the winter and spring and 4°C in the summer and autumn. They also examined the wind influence on NYC's UHI. Winds contribute to the vertical mixing of air columns and the ventilation of the city and play an important role in the spatial evolution and magnitude of the UHI. At midnight, ΔT_{UHI} (defined as urban temperatures minus inland rural temperatures) averages 4.8°C when the wind speed is less than 2.5 m s^{-1} but only 2.1°C when the wind speed is above 7.5 m s^{-1}. Wind direction has a profound influence on the magnitude and location of New York City's UHI because of its coastal setting. When wind blows from the west (from land), ΔT_{UHI} is significantly larger. When the wind has an easterly component, it comes off the relatively colder water and tends to cool the city. It was noted that sea-breeze southerly winds penetrating from Long Island's south shore often provide greater cooling than sea-breeze winds coming off the New Jersey shoreline (Gedzelman et al. 2003). Gedzelman et al. (2003) found that the sea breeze often provided relief to NYC during a multiday spring heat wave, but the work did not include summertime heat wave events.

Coastal megacities like NYC experience complex atmospheric circulations involving the interaction of UHI's with regional maritime and continental air masses. For example, there is the sea-breeze system, a circulation forced by atmospheric pressure differences that develop as a result of the different solar absorption properties of

sea and land (Miller et al. 2003). The horizontal thermal contrast between cool marine air and warm continental air is often sharp and takes on frontal characteristics (Zhong and Takle 1992; Miller et al. 2003; Orton et al. 2010). The land–sea temperature contrast of the New York City region is well documented (Thompson et al. 2007; Pullen et al. 2007; Orton et al. 2010). Multiple sea-breeze boundaries have been identified in the NYC metropolitan area: over Brooklyn and Queens, along the coast of Long Island Sound, and near the harbor area (Novak and Colle 2006; Thompson et al. 2007). During evenings with strong sea breezes present the heat island starts somewhat later and increases more slowly yet still approaches similar amplitude after midnight (Gedzelman et al. 2003).

Modeling the complex urban–coastal atmospheric environment of the NYC metropolitan region constitutes a significant challenge. It is complicated by 1) the extreme horizontal and vertical variability of the urban landscape (e.g., skyscrapers), 2) the variety of surface forcings (e.g., land-use categories), and 3) the presence of coastal discontinuities and coastal circulations (Holt and Pullen. 2007). Our long-term goal is to couple specialized models (e.g., ocean, dispersion, land cover, and an urban canopy parameterization) to continuously work on fine-tuning the underlying parameters, and to run our models at sufficiently high resolutions, in order to improve NYC's atmospheric forecasts.

This paper focuses on observations, forecasts, and forecast evaluations for two extreme heat events in the summer of 2011, as well as the impact of the UHI and sea-breeze circulation on these events. We use two models and networks of observations to analyze extreme temperature forecasts for the NYC metropolitan environment: the Naval Research Laboratory Coupled Ocean–Atmosphere Mesoscale Prediction System (COAMPS[1]) centered over the NYC metropolitan area and the Weather Research and Forecasting (WRF) North American Mesoscale (NAM) domain, as well as regional land- and coast-based sensor networks (available through the NYCMetNet website; http://nycmetnet.ccny.cuny.edu/), all of which are discussed in detail in section 2. We evaluate the ability of the models to capture the interaction between the urbanized region and the atmosphere, with a particular focus on the sensitivity of the models in relation to urban–coastal circulation features. Final suggestions and improvements to models will be mentioned in the concluding section. This study contributes to the scientific understanding of local atmospheric circulations influenced by the urbanization of coastal regions. It also compares a dense network of land-based observations with models, which can help improve forecasts for complex urbanized regions.

[1] COAMPS is a registered trademark of the Naval Research Laboratory.

2. Methods

The two most extreme heat events that impacted the NYC metropolitan region in 2011 are the focus of this paper, occurring during 7–9 June and 21–23 July (Fig. 2). Although for the purpose of warning the public of extreme heat events, the National Weather Service uses the heat index, defined in terms of relative humidity and temperature (http://www.nws.noaa.gov/os/heat/index.shtml), here, an "extreme heat event" is defined as having a maximum daily temperature greater than 32.2°C (90°F) for three or more consecutive days, a common regional definition for a heat wave in the northeastern United States (e.g., NYC Office of Emergency Management; Rosenzweig et al. 2009). In section 3, we examine the accuracy of model forecasts for the early morning temperatures that followed the hottest days. Urban–rural temperature differences usually disappear by midday when ambient temperature increases; hence, it is important for the study to look into the more pronounced temperature differences that occur during early morning periods. The warmest early morning temperatures (0000–0600 EDT) were those of 8–10 June and 22–24 July, so while the extreme heat events by definition were 7–9 June and 21–23 July, this paper predominately focuses on these mornings.

a. Summary of two extreme heat events

During both events, synoptic conditions were representative of typical extreme heat events in NYC with clear skies and a low pressure system to the north [National Oceanic and Atmospheric Administration (NOAA) Central Library U.S. Daily Weather Maps Project: www.hpc.ncep.noaa.gov/dailywxmap/]. The cyclonic flow around the low pressure system brought westerly winds to NYC, and on several days this deflected the southerly sea breeze somewhat eastward, preventing maritime air from penetrating into the city from the south.

The June heat event was associated with a slow-moving surface low pressure system that moved across the north-central section of the country, past the Great Lakes, and to the East Coast over 4 days, with record-breaking temperatures exceeding 37.8°C (100°F). High pressure built in to the south and low pressure approached from the northwest, bringing west winds and keeping the sea breeze from penetrating deep into NYC. The system was displaced by a cold front that moved through NYC during the evening of 9 June with north

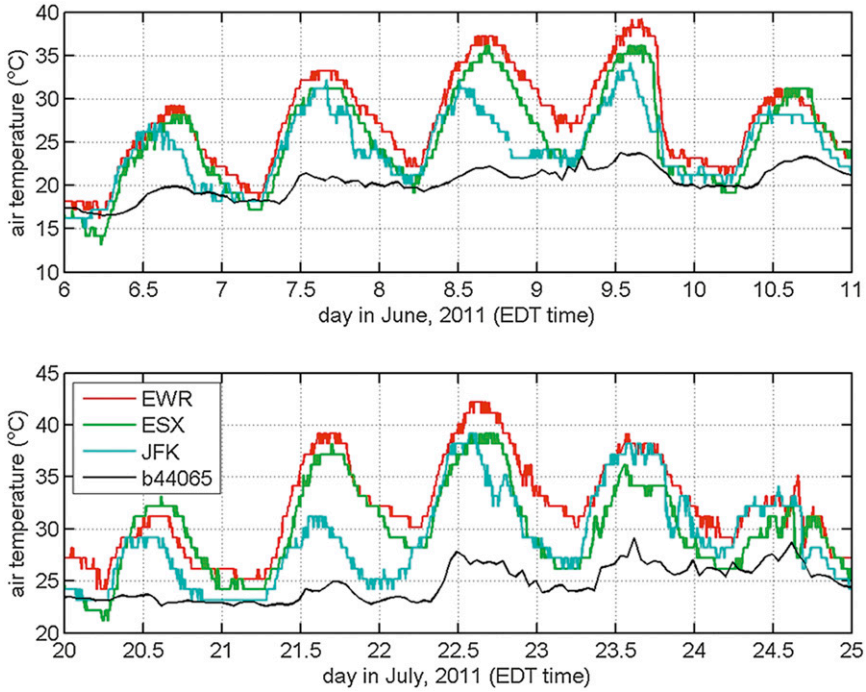

FIG. 2. Air temperatures measured at NYC regional airports and a coastal ocean buoy (NDBC buoy 44065, 22 km south of Long Island): (top) June and (bottom) July 2011.

winds and cooler, drier air. The event had one day with strong maritime air influences in NYC, with a sea breeze pushing deep into the city and bringing cooler temperatures on 8 June, which will be examined in more detail in this paper.

The July heat event began with a large, deep ridge of high pressure covering the central United States in mid-July. This pulled hot humid air in from the Gulf of Mexico and southern United States, and then spread slowly eastward, with low pressure building over southeastern Canada. On 22 July an all-time record high temperature was set at Newark Liberty International Airport (EWR) of 42.2°C. The event was also noteworthy across the country for its dangerously hot daily low temperatures that were often over 27°C. The July heat wave, the hotter of the two events, created the largest recorded energy load on the local grid (B. Hertell, Consolidated Edison Company of New York, 2011, personal communication), likely due to extensive air conditioning use. The event ended in NYC with the arrival of a cold front around midday on 24 July, and a cooler air mass and high pressure building in from the northwest.

b. *COAMPS numerical model*

In the present study the nonhydrostatic COAMPS system, a numerical weather prediction model (Hodur 1997), is nested down to 333-m resolution (five nests; Fig. 1), centered on the island of Manhattan. The outer grid's atmospheric forcing is derived from the Navy Operational Global Atmospheric Prediction System (NOGAPS). Here, we will only present results for the 1000-m resolution, 91 × 91 point grid, which covers the New York metropolitan area; the 333-m grid only covers the center of the city, so is not as useful for studying coastal or heat island effects.

In this configuration, COAMPS uses 60 vertical sigma levels, with 30 levels in the lowest 1200 m (and 13 in the lowest 100 m) to allow for greater resolution of boundary layer processes (Holt and Pullen. 2007; Thompson et al. 2007). The model has been run twice per day in real time since 2010 (https://cavu.nrlmry.navy.mil/COAMPSOS/). Hourly output is used for the study of the heat events, where the second 12 h of each 24-h prediction cycle is utilized to conservatively avoid any spinup issues. All forecasts use the previous COAMPS 12-h forecast as a first guess, blended with observations using a three-dimensional variational technique.

The model is run with surface boundary forcing for the ocean from an ocean-state analysis, for vegetated and nonurban areas using the Noah land surface model (LSM; Liu et al. 2006) and for urban areas using an urban canopy (UCP) parameterization scheme. Specifically, the ocean boundary condition forcing is from the Navy Coastal Ocean Data Assimilation (NCODA) 9-km

multivariate optimum interpolation ocean-state analysis that combines in situ and remotely sensed data to give highly accurate sea surface temperature estimates (Cummings 2005). The UCP incorporates the effects of the city morphology and heating to obtain a more realistic representation of the diurnal evolution of the UHI. This multilayer scheme is based on the Urban Canopy Model of Brown and Williams (1998; BW-UCM), which was later modified to include a rooftop energy equation by Chin et al. (2005). The UCP includes momentum loss, turbulence production, radiation absorption, and a surface energy budget, all accompanied by specific parameters for NYC. The UCP and its settings are described in more detail in Holt and Pullen (2007). Land classification inputs into the UCP come from a detailed database of land surface characteristics derived from the 1992/93 WRF (U.S. Geological Survey, USGS) 24-category, 1-km dataset, combined with a gridded 250-m resolution local database for Manhattan (Burian et al. 2005).

c. *NAM numerical model*

The North American Mesoscale Forecasting System (NAM) is one of the primary models of the National Weather Service Environmental Modeling Center and supplies mesoscale forecasts to public and private sector meteorologists (http://www.emc.ncep.noaa.gov). The NAM forecasting system encompasses multiple daily runs of the weather research and forecasting non-WRF hydrosystatic mesoscale model for the United States at 12-km resolution, beginning in 2006 (Janjić et al. 2001, 2005). NAM uses 60 sigma-pressure hybrid levels (similar to COAMPS's 60 sigma-z levels), but these are spaced more broadly than those in COAMPS throughout the planetary boundary layer. The Noah LSM, implemented in 2004 (Chen and Dudhia 2001; Ek et al. 2003), also provides surface sensible and latent heat fluxes, as well as surface skin temperature, as lower boundary conditions to the WRF model as is done for COAMPS. While NAM recognizes the presence of urban land and its boundaries through the specification of high-density residential land use, it uses a bulk transfer scheme in which the characteristics of urban surfaces are parameterized in Noah (Liu et al. 2006). A website (http://gcmd.nasa.gov/records/NOAA_NOAH.html) provides further description of the land surface types and parameters being fed into the WRF model maintained by the operational community of the Developmental Testbed Center (DTC; http://www.dtcenter.org/).

d. *Observational datasets*

The observational data used for verification purposes come from a variety of sources, all collected on NYCMetNet, a website with hundreds of meteorological sites around the NYC metropolitan area and supported by the Optical Remote Sensing Laboratory (ORSL) of the City College of New York. Specific meteorological stations highlighted in this paper are managed by Weatherflow Inc., UrbaNet (a public–private partnership with NOAA's Air Resources Laboratory and Earth Networks, Inc.), the Automatic Position Reporting System as a Weather Network (APRSWXNET, which is a citizen-observer program), the National Weather Service's Automated Surface Observing System (NWS-ASOS), and Earth Networks (WeatherBug). As such, the data are from a variety of private and governmental meteorological stations, with some diversity in sensor height and placement. The sensor heights range from the nominal 10-m height above ground level [an automatic weather station standard according to the World Meteorological Organization (Oke 2006)] or on the top of buildings at various heights above roof level. All data have been quality controlled in time series form, by histogram, and also by cluster analysis of temperature to locate any clear outliers. The entire breadth of the data sources listed above are utilized for temperature, whereas only NWS-ASOS and Weatherflow stations are utilized for wind data presented in this paper. The Weatherflow data are from seashore-based meteorological stations with no wind obstructions and, thus, are highly valuable in measuring coastal winds.

3. Results and discussion

Model forecasts and observations are compared first qualitatively in spatial terms (section 3a), with particular emphasis on the UHI pattern and early morning temperature. The UHI is defined similarly to the approach used by Gedzelman et al. (2003), where we contrast urban and rural inland temperatures, omitting coastal stations that reflect seasonally varying sea surface temperatures. Then in section 3b, the temperature forecasts are evaluated statistically for airport meteorological stations and for general zones across the region including several stations each in rural, central urban, coastal urban, and coastal suburban areas. Wind and temperature evolution patterns are examined in more detail in section 3c for a central day of each heat wave (8 June and 22 July), both of which were followed by the event's highest low temperature in the early morning hours. Finally, the wind forecasts are evaluated statistically against NWS-ASOS and Weatherflow stations (section 3d).

a. *Average early morning temperatures and the urban heat island*

The average near-surface early morning temperatures were mapped across the region to capture qualitative

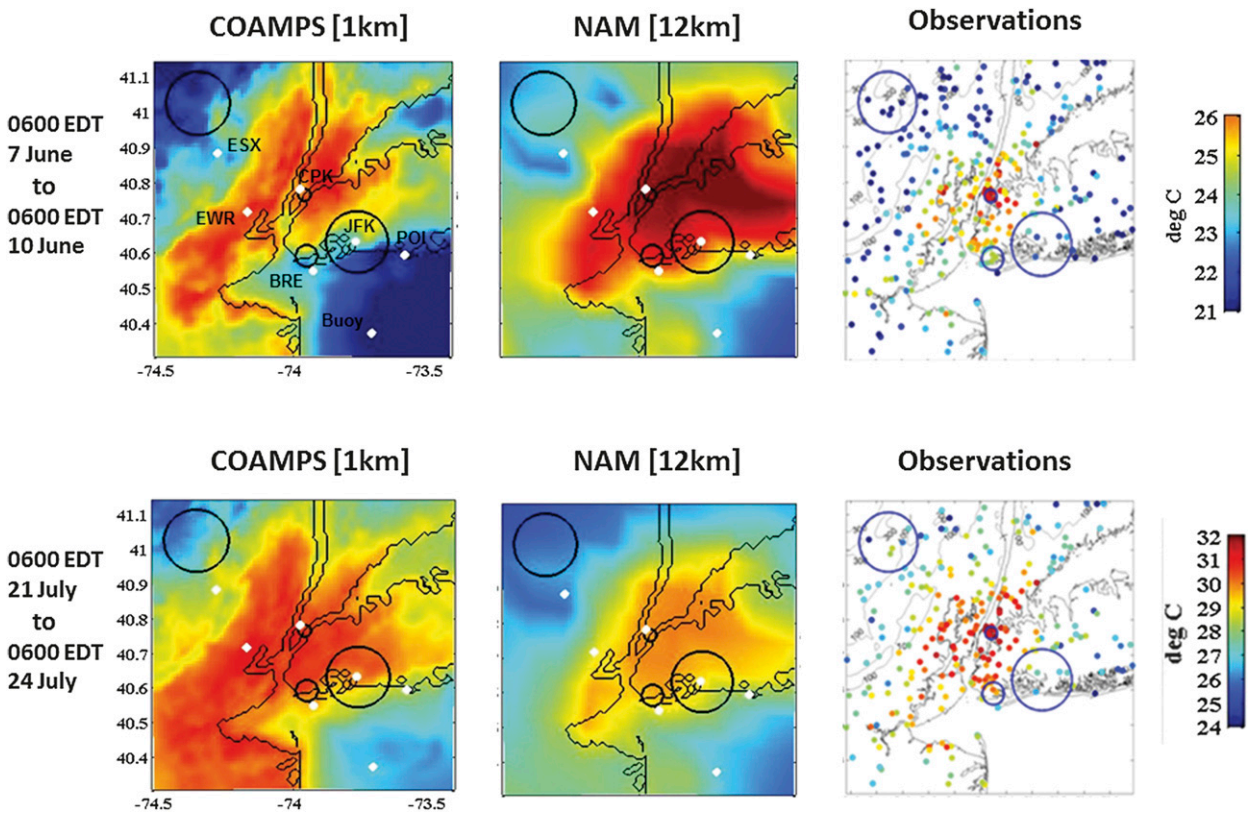

FIG. 3. Mean early morning (0000–0600 EDT) near-surface (10 m) air temperatures for (from left to right) COAMPS, NAM, and observations during the two extreme heat events: (top) 7–10 Jun and (bottom) 21–24 Jul. The circles represent zones for additional comparisons. Note the different temperature color scales for the two events.

similarities and differences among the models and observations (Fig. 3). Hourly temperature values were averaged from midnight to 0600 local time (eastern daylight time, EDT) for all sources: NAM, COAMPS, and the observations. First, focusing on an event-to-event comparison in the observations and model results, July's heat wave had higher observed temperatures over a broader spatial extent than did the June event (Fig. 3, right). The urban heat island temperature difference (ΔT_{UHI}) inferred from comparing temperatures on the western edge of the grid to those in the city center (center of COAMPS grid 4; Fig. 1) is approximately 4°–5°C for both events. This is consistent or slightly higher than the 4°C summer ΔT_{UHI} average of Gedzelman et al. (2003). While the heat event was exacerbated by the UHI, the UHI effect was not amplified substantially over the average ΔT_{UHI} levels found in other studies [such as Gedzelman et al. (2003) and Bornstein (1968)]. COAMPS

TABLE 1. June heat event statistics for airports and four zones (shown in Fig. 3). Bias is calculated as a mean difference: model minus observed temperatures.

Mean near-surface air temperatures (°C) statistics, early morning average (0000–0600 LT 8–10 Jun 2011)										
	Obs		COAMPS				NAM			
Station	Mean	Std dev	Mean	Mean bias	Std dev	RMSE	Mean	Mean bias	Std dev	RMSE
Essex County Airport	22.25°	2.22°	22.59°	0.34°	3.04°	2.65°	22.70°	0.45°	2.10°	2.48°
EWR	25.08°	2.96°	25.20°	0.12°	3.63°	1.96°	25.17°	0.09°	1.70°	2.34°
JFK	22.05°	1.26°	23.25°	1.20°	1.82°	2.21°	25.14°	3.09°	1.79°	4.52°
Rural zone	20.93°	1.91°	22.33°	1.4°	3.16°	1.75°	22.87°	1.94°	2.22°	2.83°
Urban zone	25.57°	2.93°	24.75°	−0.82°	3.28°	1.93°	25.90°	0.33°	1.73°	2.74°
Coastal urban zone	23.86°	2.62°	23.78°	−0.08°	1.95°	1.62°	25.43°	1.57°	1.78°	3.63°
Coastal suburban zone	22.57°	1.64°	24.06°	1.49°	2.09°	2.43°	25.49°	2.92°	1.87°	4.02°

TABLE 2. As in Table 1, but for the July heat event.

Mean near-surface air temperatures (°C) statistics, early morning average (0000–0600 LT 22–24 Jul 2011)										
	Obs		COAMPS				NAM			
Station	Mean	Std dev	Mean	Mean bias	Std dev	RMSE	Mean	Mean bias	Std dev	RMSE
Essex County Airport	27.50	1.51	28.63	1.13	0.96	1.89	26.14	−1.36	0.89	1.85
EWR	30.74	1.15	31.04	0.3	1.21	2.19	28.83	−1.91	1.08	2.01
JFK	27.21	1.57	29.87	2.66	2.38	3.03	29.21	2.0	1.39	3.01
Rural zone	26.18	1.63	27.35	1.17	1.78	1.88	25.93	−0.25	0.69	1.86
Urban zone	31.03	1.26	30.42	−0.61	1.28	1.14	29.83	−1.2	0.96	1.03
Coastal urban zone	29.79	1.23	30.25	0.46	2.15	0.87	29.43	−0.36	1.34	1.01
Coastal suburban zone	27.28	1.63	30.58	3.3	2.07	2.92	29.65	2.37	1.39	3.01

predicted a similar spatial pattern for both events, with more elevated temperatures in July.

Second, focusing on model-to-observation comparisons, spatial temperature distribution patterns vary among the models and observations. COAMPS produces a spatial maximum temperature that is located north of the city center and extends toward the northeast and southwest along the urbanized corridor. NAM predicts a large UHI centered on western Long Island, with very little coastal cooling evident along Long Island's south shore and none around Long Island Sound. It is interesting to note and compare the overall magnitude of the UHI (as represented by ΔT_{UHI}) as well as the spatial extent of the UHI effect (i.e., how widespread in

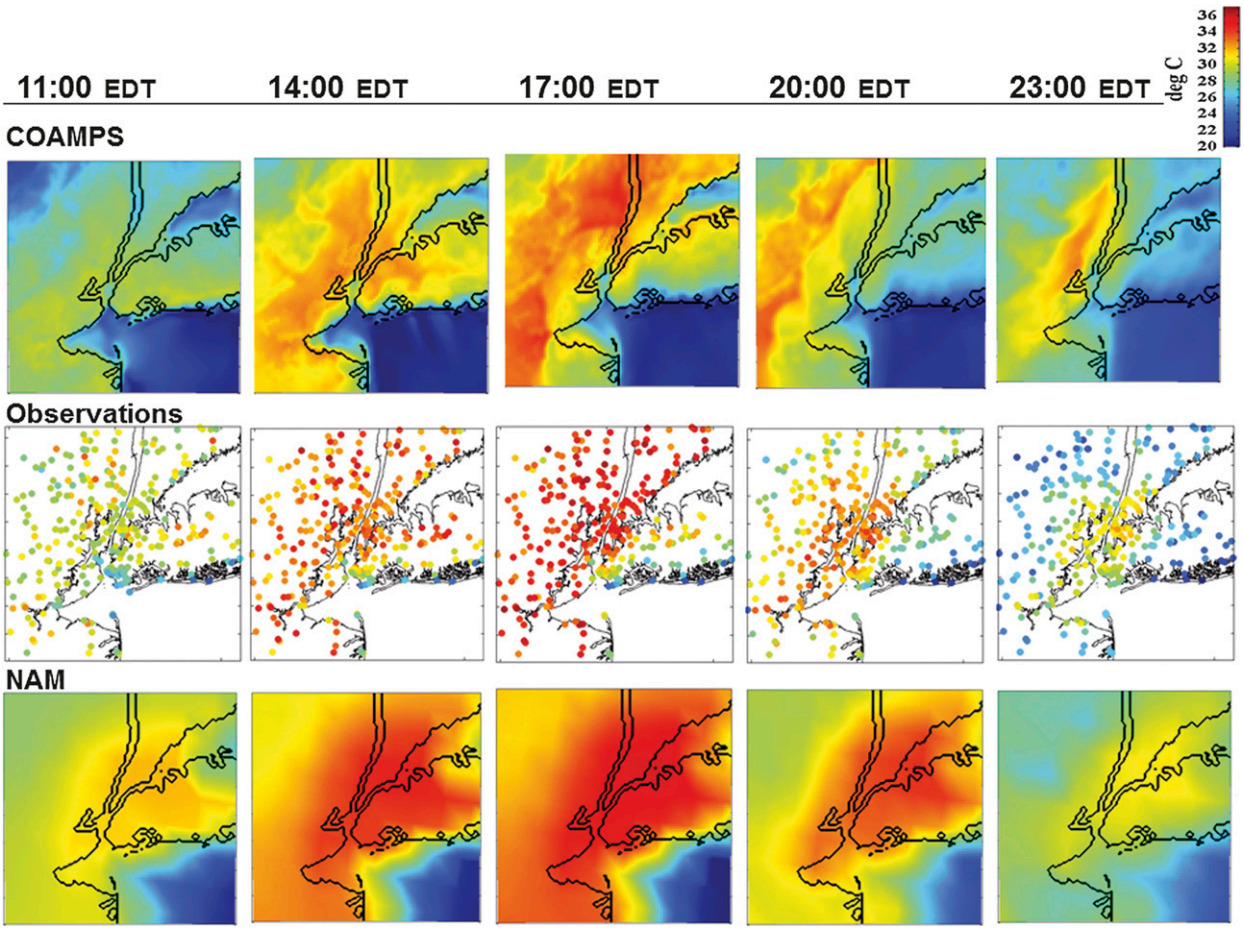

FIG. 4. Three-hourly evolution of near-surface air temperature covering 1100–2300 EDT 8 Jun for (top to bottom) COAMPS, observations, and NAM.

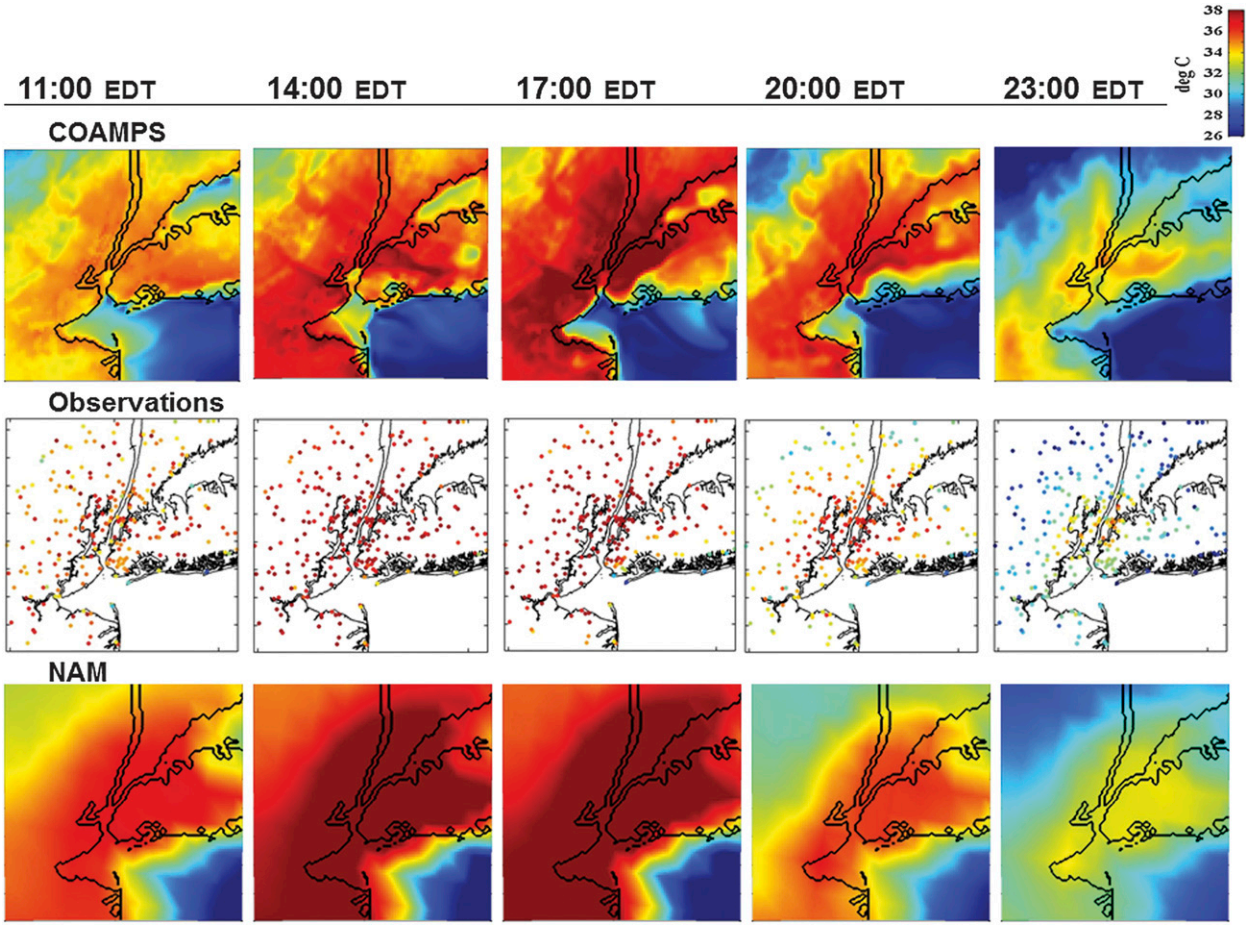

FIG. 5. As in Fig. 4, but for near-surface air temperature covering 1100–2300 EDT 22 Jul.

space it is). Compared to observations, both models spatially overextend their high heat area: NAM particularly north of the city and eastward onto Long Island, and COAMPS north of the city and toward the west and southwest. In general, the COAMPS prediction of ΔT_{UHI} is more consistent with the observations than is the NAM prediction of ΔT_{UHI}; however, there are many subtleties worth discussing regarding the spatial inhomogeneity of the horizontal temperature profiles and this has inspired the definition of zones as introduced in sections 3b below.

COAMPS overestimates temperatures on the southwestern edge of the urban region (40.6°N, 74.4°W) and also on the northwestern edge (40.95°N, 74.05°W), which leads to an inaccurate extension of the UHI to the southwest and north (Fig. 3, left). A brief review of the land-use database used for the COAMPS model runs shows that these two regions are identified as "urban," whereas satellite visible imagery reveal these to be well-forested suburban areas. Subsequent model runs with the land-use data converted from urban to forest lead to a decrease in nighttime temperature of 3°–4°C, demonstrating the impact of land surface characterization on near-surface temperatures in these locations.

b. *Temperature forecast statistics: Stations and zones*

We present two approaches to comparing the temperatures. The first uses local airport meteorological stations, and the second uses a zone comparison of rural–urban–coastal regions by grouping stations into clusters (zones; labeled in Fig. 3). The zone-based approach is intended to enable a better comparison of models to observations, as it suppresses inconsistencies in any particular station, such as in the case of airports. The zone analysis uses four circular hubs that were chosen to represent distinct microclimatic interest areas. Three of the zones lie on a transect line running from coastal to urban to rural environments; a fourth zone was added out of our interest in analyzing an additional coastal area around NYC. The rural circle is a 9.5-km radius located in the northwest corner of the grid at latitude 41.02°, longitude −73.76°. The urban circle is

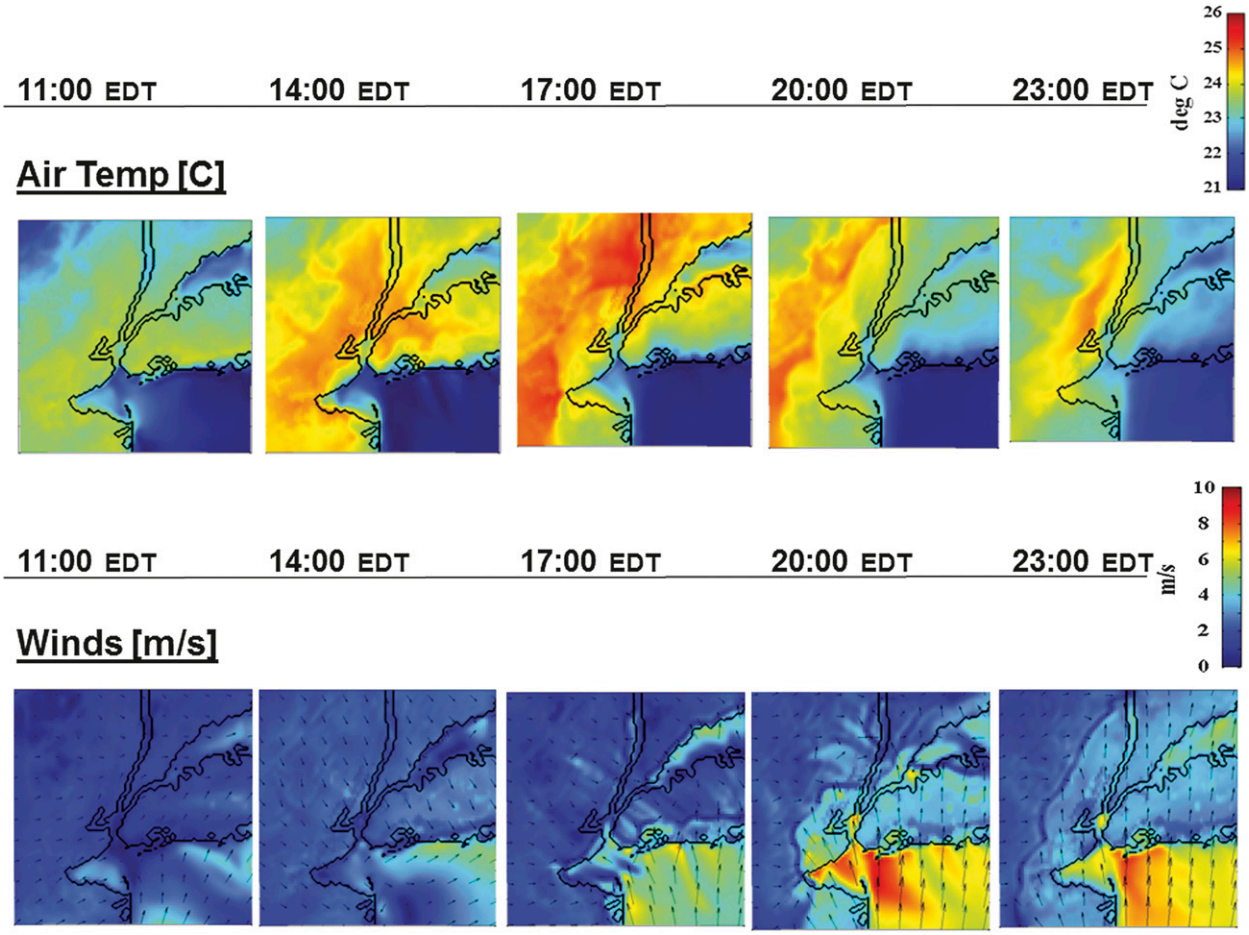

FIG. 6. Three-hourly evolution of COAMPS (top) near-surface air temperature and (bottom) wind during 1100–2300 EDT 8 Jun.

2 km in size and located in midtown Manhattan and Queens with latitude 40.76°, longitude −73.95°. The two coastal circles are to the east of the city over downtown Brooklyn and farther into Long Island in the vicinity of John F. Kennedy International Airport (JFK): 3.5-km radius, latitude −73.95°, longitude 40.59°; 9.7-km radius latitude −73.76°, longitude 40.62°. Each of the four selected hubs contains a sample of six observational stations that are mirrored into model indices.

Tables 1 and 2 summarize the temperature values for both heat events. Examining model performance broadly over both heat events, COAMPS temperature biases were small in most cases, with station or zone mean biases of less than 1.2°C in 78% of cases. NAM had far fewer cases with mean biases below 1.2°C (only 43% of cases). In terms of statistics at three of the region's airport meteorological stations, both models had small mean bias values for the rural airport (Essex) and the urban airport (Newark). The coastal airport (JFK) was harder to match under both the June and July events. The COAMPS mean bias was 1.20°C (3.09°C for NAM) during the June event and over 2.66°C (2.0°C for NAM) during July's. Likewise, RMSEs were larger primarily at JFK, the coastal airport.

COAMPS best captures the temperature conditions over the coastal–urban zone. It has its lowest mean bias of −0.8°C and an RMSE of 1.6°C for June, with a bias of 0.46°C and an RMSE of 0.87°C for July (Tables 1 and 2). This provides a positive indication of COAMPS's ability to represent the unique dynamics of coastal–urban regions. Over the rural zone COAMPS's performance is relatively poor with mean biases of 1.17°C for June and 1.4°C for July. COAMPS's low performance over the rural region stems from discrepancies in land cover characteristics within the model. Discussed in more detailed previously in section 3a, COAMPS classifies the region as urban land cover against the true forest-like landscape, hence predicting higher temperatures than observations. NAM maintained similar standard deviation values for three out of the four zones, with the exception of the coastal zone. Both models give less favorable results along the coastal area of Long Island

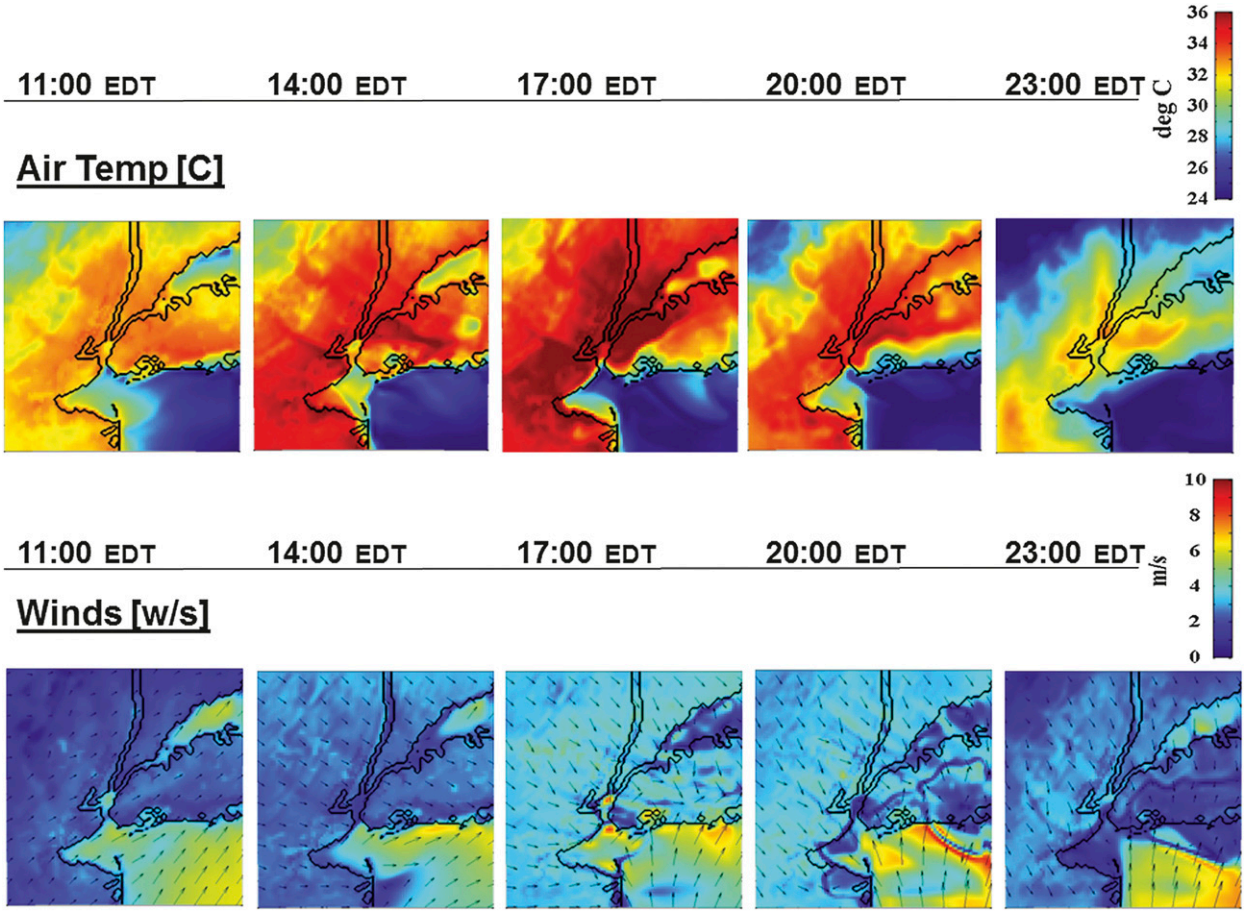

FIG. 7. As in Fig. 6, but covering 1100–2300 EDT 22 Jul.

(coastal zone): COAMPS yielding 1.49° and 3.3°C mean biases for June and July, respectively, and NAM with 2.92° and 2.37°C for June and July, respectively. Large RMSEs are calculated for both models during both events for this region.

c. *Diurnal cycle of air temperatures and wind*

A late afternoon sea breeze blowing across the coastal zone can mitigate extreme heat, bringing a large drop in air temperatures. The ventilation of the city by the sea breeze during the June and July events is shown in Figs. 4–7, which show the temperature evolution over 12-h periods across the metropolitan area. For both heat events, the coastline temperature gradient is evident, both in the observations and from COAMPS. NAM, likely due to its lower model resolution, does not accurately forecast temperature gradients over Long Island's coastlines and the inner New York Bight.

For the June event, observations show that areas near the southern coast of Long Island experience a consistent 3°C or greater difference compared with the urban center, reaching as high as 15°C at 1700 EDT. By 1700 EDT a sea-breeze front develops, which is seen clearly by the COAMPS predictions in Fig. 6. Wind direction switches from westerly to southerly and continues to intensify from 4 to 10 m s^{-1} along certain regions of Long Island's south shore. The sea breeze cools the region east of NYC. From 1700 EDT onward, COAMPS predictions erroneously extend sea-breeze-driven evening temperature relief across the entire city, whereas observations show that the UHI maintains its hold over the city (Fig. 4).

July's heat event represented in Fig. 5 also shows a pronounced difference of ~10°C between temperatures in the urban core versus the south shore of Long Island by 1700 EDT. However, the cooler coastal temperatures are limited to the barrier islands and do not extend northward onto Long Island like they did in June. The gradient from the urban core out onto Long Island presents a delayed but also very strong temperature difference (~5°C by 2300 EDT). This difference is present west of the city, suggesting it is primarily a UHI

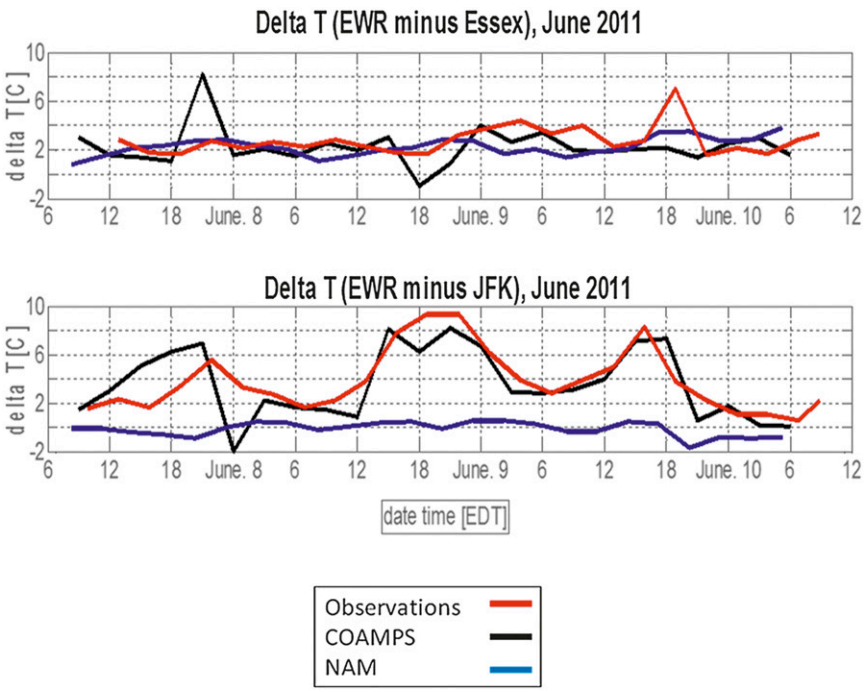

FIG. 8. Modeled and observed ΔT, defined as the urban temperature (EWR) minus the "external," nonurban temperature, for the June 2011 heat event. (top) Essex County Airport represents a rural, inland station. (bottom) JFK represents a coastal station.

effect instead of a maritime sea-breeze effect. Sea-breeze fronts are insubstantial until 2000 EDT and remain constrained to areas farther out into Long Island where water temperatures are cooler in comparison to harbor waters. COAMPS develops southerly winds over the coastal ocean by 1700 EDT for both events, but the marine cooling only penetrates a small distance onto Long Island for the July event (Fig. 5) and sea-breeze winds there generally remain weak (Fig. 7). COAMPS slightly exaggerates the cooling over southern Long Island and Brooklyn, relative to the observations.

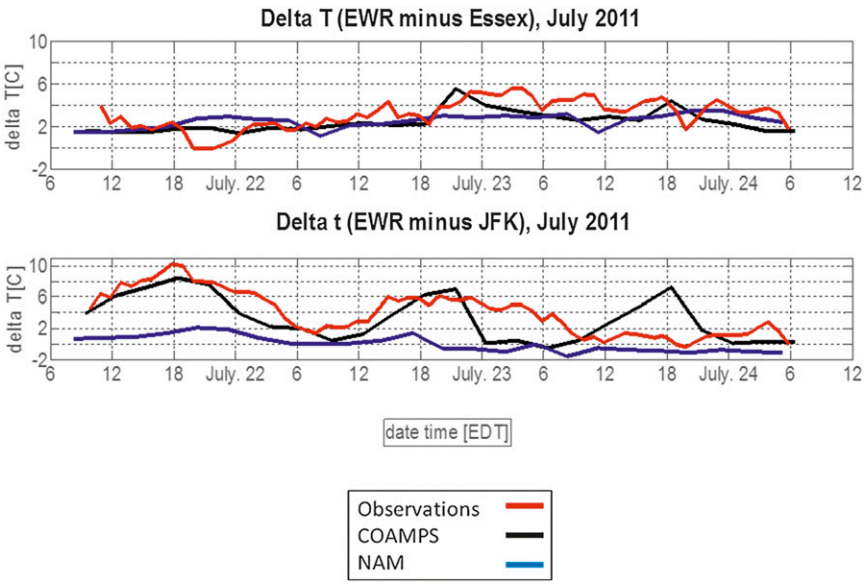

FIG. 9. As in Fig. 8, but for the July heat event.

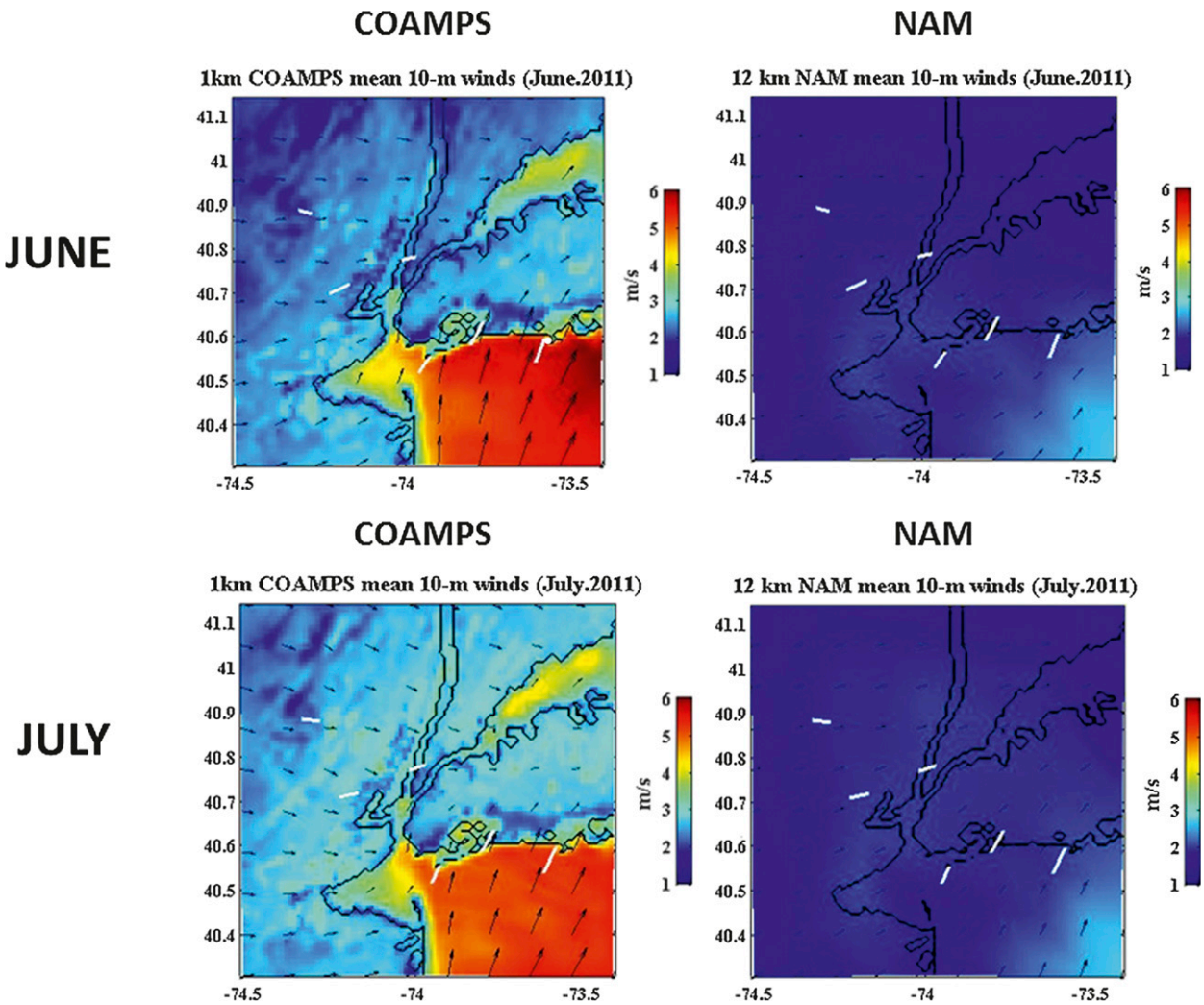

FIG. 10. Mean 10-m winds for (left) COAMPS and (right) NAM during the (top) June and (bottom) July heat events. Observed stations' wind velocity and direction are shown with white lines.

The stronger observed sea-breeze cooling of NYC in June, relative to July, did not appear to be caused by a greater maritime–continental air temperature gradient. The difference between the maritime and continental air temperatures reflects the physical forcing for the sea breeze (Miller et al. 2003), and these differences were strong and similar for both heat waves. For the June event, the temperature difference during the mid-afternoon between Newark's airport and buoy 44025, located 22 km southeast of New York Bright's apex, was 13°–15°C. For the July event, it was 12°–14°C, only about 1° lower. It is clear that such a strong temperature difference is sufficient to set up a sea-breeze circulation, so other forces must be at work if the sea breeze had reduced inland penetration in July. The difference in the two days is likely caused by differences in synoptic forcing; surface isobar maps show a meridional pressure gradient across the New York City region of $\sim 7 \times 10^{-6}\,\mathrm{mb\,m^{-1}}$ at 0700 EDT 8 June, while it is 50% higher, at $1.1 \times 10^{-5}\,\mathrm{mb\,m^{-1}}$, at 0700 EDT 22 July. The difference in synoptic forcing is also reflected in COAMPS surface winds for inland regions shown in Figs. 6 and 7, with moderate northwest winds dominating for the July event and weak winds for the June event. Comparisons of COAMPS and observed SST at buoy 44065 show a mean model bias of −0.84°C and an RMS error of 1.50°C for June, with a mean bias of 0.03° and a 0.99°C RMS error for July. The success of the COAMPS predictions of SST over the coastal ocean may help explain the model's strong performance in forecasting coastal atmospheric dynamics, such as the sea breeze.

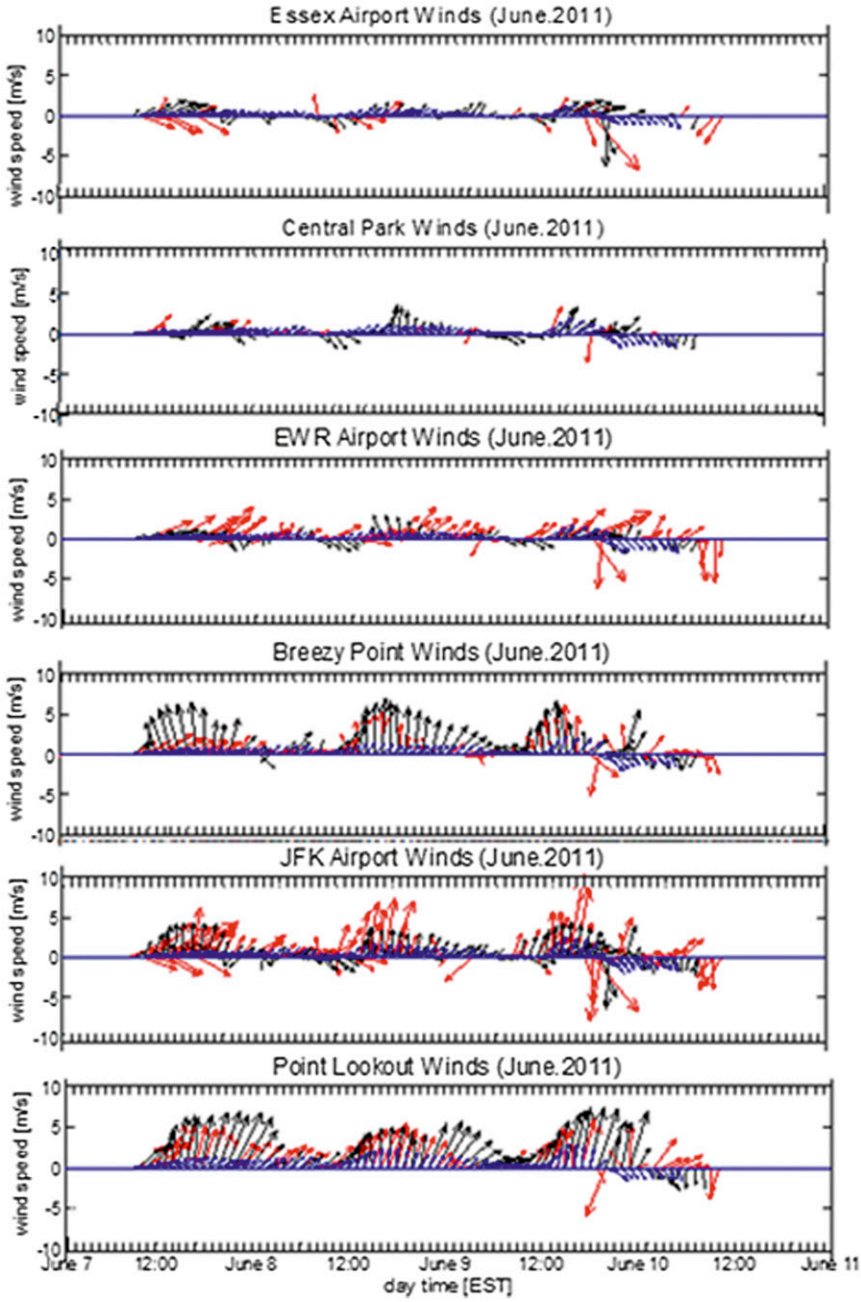

FIG. 11. Wind vectors during the June heat event: observations (red), COAMPS (black), and NAM (blue).

We next investigate the impact of diurnal cycles on the urban–rural and urban–coastal temperature gradients, defined as ΔT_{UHI} and $\Delta T_{\mathrm{coastal}}$ (ΔT referring to urban minus nonurban near-surface temperature). Figures 8 and 9 show the ΔT time series comparisons for airport stations for both June and July's heat events. Gedzelman et al. (2003) showed typical diurnal cycling in the UHI from 0° to 4°C, and found that it was larger on clear nights with low humidity and northwest winds. Here, we see a UHI that had little diurnal cycling and intensified as each event progressed, with maximal values of 4°–6°C.

For the June event, a diurnally varying gradient is strongly present at the coastlines (EWR minus JFK) while absent farther inland (EWR minus Essex) (Fig. 8). Observations capture a nearly 10°C difference between

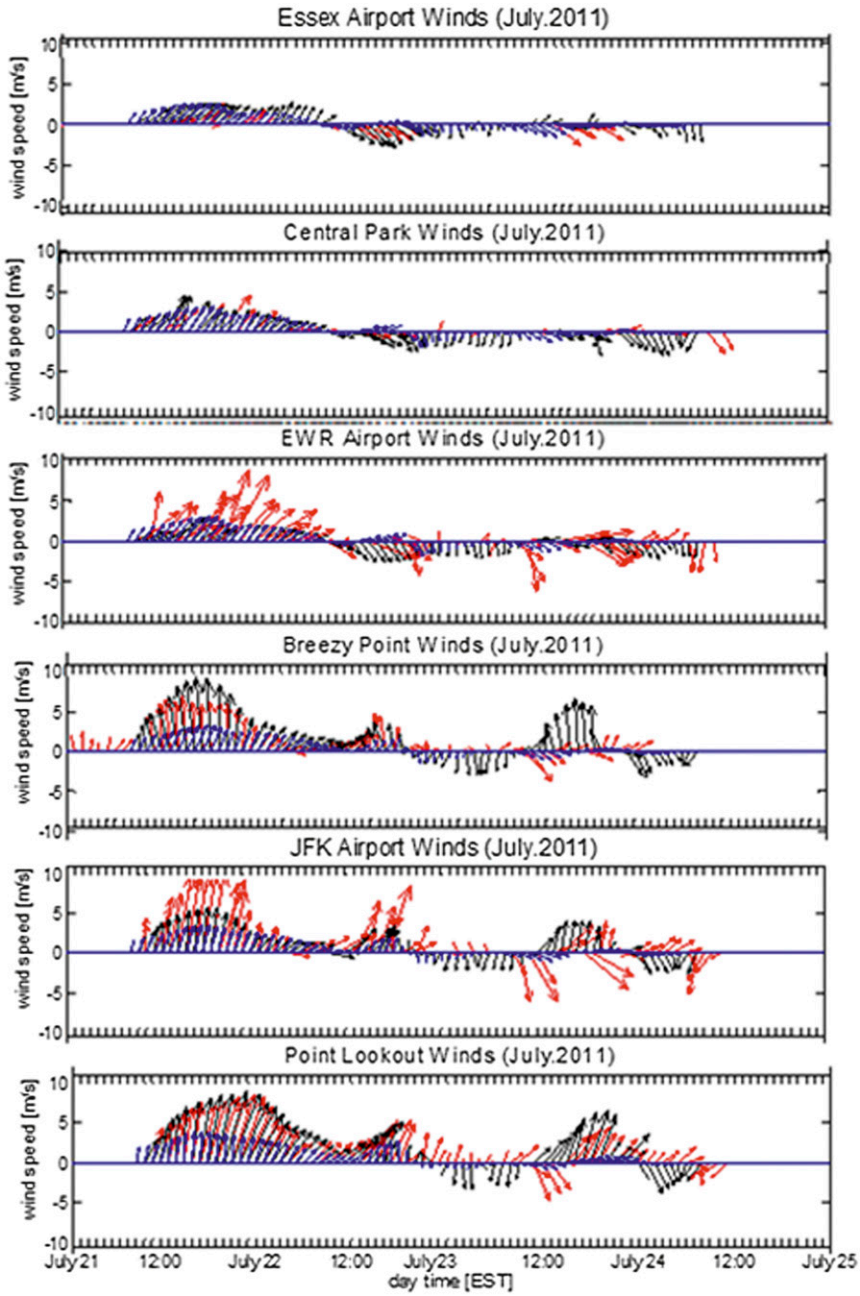

FIG. 12. As in Fig. 11, but for the July heat event.

urban EWR and coastal JFK during evening hours following the June event's hottest day, the 8th (Fig. 8b). This temperature difference then lessens to 3.0°C by the early morning hours. In comparison, the ΔT_{UHI} remains relatively constant throughout the duration of the heat event, typically ranging from 2° to 4°C (omitting late on 9 June, when a front was passing and led to a spike). COAMPS agrees with observations well, reproducing the effect of the northward penetration of cooler air by the sea breeze. NAM appears not to develop a sea breeze at all for this event, perhaps due to insufficiently cool ocean temperatures or due to low resolution. A previous study at Chesapeake Bay by Loughner et al. (2011) found that a 4.5-km resolution was sufficient for modeling ground-level ozone dynamics, whereas the 13.5-km resolution version of their model did not capture ground-level pollutants across the coastline. These results suggest resolution-dependent challenges in

TABLE 3. Wind speed ($m\,s^{-1}$) statistics for 7–10 Jun 2011.

	Obs		COAMPS				NAM			
Station	Mean	Std dev	Mean	Mean bias	Std dev	RMSE	Mean	Mean bias	Std dev	RMSE
Essex County Airport	3.13	1.74	3.08	−0.05	1.42	1.81	2.20	−0.93	0.54	1.85
Central Park	2.76	1.21	2.43	−0.33	1.08	0.99	2.13	−0.63	0.49	1.13
EWR	4.18	1.88	2.16	−2.02	0.88	2.54	1.98	−1.64	0.52	2.76
Breezy Point	3.17	1.14	3.87	0.7	1.60	1.48	1.99	−1.18	0.43	1.59
JFK	4.45	2.06	2.9	−1.55	1.01	2.28	1.96	−2.49	0.39	3.25
Point Lookout	3.75	1.53	4.63	0.88	1.82	1.85	2.02	−1.73	0.36	2.27

simulating temperature gradients along coastlines for initiating sea-breeze dynamics. Such resolution restrictions are similarly found in this study.

Based on $\Delta T_{\mathrm{coastal}}$ (Fig. 9) for the July event, considerable sea-breeze effects exist on the 21st, but decrease each consecutive day. COAMPS has prediction errors during the later days of the event (23–24 July) where the model overestimates the sea-breeze cooling effect on Long Island's south shore. NAM predicts a $\Delta T_{\mathrm{coastal}}$ from −2° to 2°C throughout, with barely detectable diurnal cycling. COAMPS, NAM, and the observed ΔT_{UHI} for July's event are ~2°C during the first 36 h of the event and experience a jump to ~(4°–6)°C temperature difference as the heat event continues to intensify.

The diurnal temperature range over the different regions has multiple possible causes. In this section we have investigated the coastal diurnal temperature effect influenced by local winds and the sea breeze. The mean wind patterns over the NYC metropolitan area are further analyzed below.

d. Wind forecast statistics

COAMPS and NAM's 3-day wind velocity vector averages for each heat event, superimposed with observed average values (white lines) derived from the meteorological stations, reveal the complexity of the local winds (Fig. 10). Figure 11 and 12 are wind velocity vector time series for each of the six wind stations for both June and July. Tables 3–6 show statistical assessments of the wind speed and wind direction forecasts. Scalar calculations were used for the table statistics (average, standard deviation, and RMSE), not vector calculations, taking care that wind directions were unwrapped before computing pairwise differences in the RMSEs, to avoid wraparound errors. In the computation of the mean and RMSE for wind direction we exclude weak wind cases with wind speeds below $1.5\,m\,s^{-1}$ and thus poorly defined directionality (light and variable).

Wind speeds show large standard deviations in the observations and COAMPS results (Tables 3 and 4) for coastal stations (Breezy Point, JFK and Point Lookout), reflective of the land–sea transition. All three coastal sites experience strong diurnal wind variations (Figs. 11 and 12) when compared to urban and rural stations, reflecting strong sea breezes. The COAMPS average (across stations) standard deviations were $1.30\,m\,s^{-1}$ for June and $1.25\,m\,s^{-1}$ for July. NAM winds are too weak and invariant, especially over water, with standard deviation averages of $0.45\,m\,s^{-1}$ for June and $0.79\,m\,s^{-1}$ for July in comparison to observational standard deviations of $1.59\,m\,s^{-1}$ for June and $1.81\,m\,s^{-1}$ for July. For coastal regions, wind speed patterns among the models are also noticeable through the calculated mean biases and RMSE: NAM's being generally higher than that of COAMPS at those stations. The COAMPS wind speed mean bias for both events over coastal stations is $0.89\,m\,s^{-1}$ while for NAM it is $1.36\,m\,s^{-1}$.

Winds are generally observed to be weaker over the urban and rural regions. At the Essex and Central Park stations, the COAMPS and NAM wind speed RMSE values are low. Predictions over the two airports (JFK and EWR) are the most negatively biased due to

TABLE 4. As in Table 3, but for 21–24 Jul 2011.

	Obs		COAMPS				NAM			
Stations	Mean	Std dev	Mean	Mean bias	Std dev	RMSE	Mean	Mean bias	Std dev	RMSE
Essex County Airport	2.91	1.27	3.44	0.53	0.69	0.85	2.43	−0.48	0.64	1.15
Central Park	2.63	0.83	2.87	0.24	0.87	0.92	2.11	−0.52	0.78	0.96
EWR	3.72	2.08	2.38	−1.34	0.69	2.57	1.98	−1.74	0.82	2.72
Breezy Point	2.84	1.64	4.01	1.17	1.95	1.67	2.01	−0.83	0.73	1.60
JFK	4.21	2.84	3.07	−1.14	1.15	2.38	1.97	−2.24	0.81	3.36
Point Lookout	3.95	2.17	4.44	−1.79	2.16	1.3	2.05	−1.9	0.94	2.56

TABLE 5. Wind direction (°) statistics for 7–10 Jun 2011. Data exclude conditions of light or calm wind speeds below 1.5 m s^{-1}.

Stations	Obs		COAMPS			NAM		
	Mean	Mode	Mean	Mode	RMSE	Mean	Mode	RMSE
Essex County Airport	282.2	WNW	253.3	WSW	31.67	259.6	W	30.55
Central Park	254.1	WSW	254.8	W	45.7	254.3	WSW	45.3
EWR	248.7	WSW	258.1	WSW	63.0	258.2	WSW	27.2
Breezy Point	224.7	S	197.1	S	51.6	251.1	WSW	38.2
JFK	215.6	SSW	203.4	SSW	48.9	246.1	WSW	39.6
Point Lookout	209.5	SSW	206.7	SSW	50.1	233.5	WSW	45.0

misclassification of land-use type around the airport area; COAMPS and NAM consider JFK and EWR airports to be aerodynamically ''rough'' urban surfaces, where in reality the space is relatively flat and winds are often strong, as seen from the observational time series (Figs. 11 and 12). This classification problem at airports has been observed in other studies, and can arise from the geographical reprojection of land-use data or low model resolution (e.g., Grossman-Clarke et al. 2010).

Wind direction predictions among the models show differing results for the two heat events, with June being the more successful event for both models in terms of wind direction. The COAMPS wind direction averages are 232.9° and 50° RMSE for the two events, while NAM has means of 244.6° and 45.4° RMSE for both events, compared to the observational wind direction average of 238.1°. Winds were also examined in radial histograms, and the modes (Tables 5 and 6) shows that NAM's common directional mode is from the west-southwest, while the COAMPS directional mode estimates are more variant from station to station, in better accordance with the observations. COAMPS performs best on coastal stations (JFK, Breezy Point, and Point Lookout), matching the observational wind mode of south or SSW.

4. Summary and conclusions

A study was undertaken to document and analyze the magnitude and evolution of New York City's UHI and coastal temperature gradient during two extreme heat events. While modeling such extreme events is challenging, it is an important step as urban populations continue to increase. The UHI can be a concern during heat waves due to the maintenance of high temperatures for prolonged periods, creating a potential hazard to the urban population. NYC is a coastal region that is influenced by atmospheric flows stemming from land–sea interaction; hence, complex urban environments such as NYC require detailed air–sea modeling to better simulate urban–coastal microclimates.

Observed maximum temperatures during a July event were 42.2°C at Newark's airport (an all-time record for any date), while the maximum for the June event was 39.2°C. Temperatures remained high during both events in the early morning hours (0000–0600 EDT) due to the UHI effect. Temperatures were over 30°C at many stations across the urbanized region in July, while they were above 25°C at some central urban stations in June. The early morning average UHI amplitude (urban–rural difference) for both events was 4°–5°C.

The comparison of observations to COAMPS and NAM real-time forecast models for the region during the two events has shown that atmospheric models have the ability to predict the events broadly across the coastal–urban–rural gradient. Examining model performance over both heat events and 27 sites, COAMPS has temperature RMS errors averaging 1.9°C, with that of NAM being 2.5°C. A closer look at the results shows that the COAMPS high-resolution wind and temperature predictions captured key features of the observations. While NAM approximates inland and city temperatures well, COAMPS performed better over the

TABLE 6. As in Table 1, but for 21–24 Jul 2011.

Station	Obs		COAMPS			NAM		
	Mean	Mode	Mean	Mode	RMSE	Mean	Mode	RMSE
Essex County Airport	274.8	W	260.0	SW	49.9	247.0	W	50.6
Central Park	251.2	W	267.0	NW	70.6	246.6	W	70.6
EWR	256.3	SW	279.9	WSW	50.1	251.9	SW	47.4
Breezy Point	211.5	S	189.8	S	68.4	238.2	SSW	49.9
JFK	216.7	S	212.6	S	33.2	229.5	SSW	33.0
Point Lookout	211.5	SSW	211.6	SSW	67.1	219.7	S	67.2

coastal regions. Several things are likely responsible for the higher-fidelity wind forecasts in the coastal zone, including higher resolution, better sea surface temperature estimates, and possibly also the enhanced urbanization parameterization. Zone-based statistics were not computed for winds because wind data from NYCMetNet were not utilized. One obvious reason for COAMPS relative success with the coastal wind forecasts is the 9-km resolution of the ocean state analysis used for surface forcing. Comparisons of coastal ocean temperature at a buoy 22 km southeast of New York Bight's apex [National Data Buoy Center (NDBC) buoy 44065] generally compare well with the SSTs used for COAMPS. It can be useful to resolve these small scales (or even smaller ones) in this coastal area because upwelling zones in summertime can form along New Jersey (south or southwest winds) or Long Island's south shore (west or northwest winds) and cause atmospheric cooling (Pullen et al. 2007). The higher vertical resolution of COAMPS (versus NAM) in the planetary boundary layer may also be responsible for the improved coastal winds, as this has also been shown to be important for resolving interactions between sea surface temperature and winds (Chelton and Xie 2010).

The daily evolution of near-surface air temperature across the region is influenced at times by the coastal sea-breeze phenomenon, and greater influences were observed in June versus July. Based on wind statistics for both heat events, COAMPS performs well at coastal stations. COAMPS was able to accurately forecast the heat mitigation supplied by the sea breeze, though it overpropagated the maritime air on one day. In comparison, NAM maintained a rather constant heat evolution with no effects of maritime sea breezes on the intensification of heat.

In closing, high-resolution atmospheric modeling can become an invaluable tool to manage and improve urban-coastal safety and quality of life. It is important to understand and forecast these environments at fine scales due to the numerous coastal nations that are experiencing rapid development along their coastlines. Additional efforts should therefore be made to utilize and improve computer models for NYC and other coastal metropolitan areas, to further understand and predict their meteorological complexities.

Acknowledgments. Two of the authors (TH and WTT) were supported by Office of Naval Research Program Element 0601153N. We are grateful to Jay Titlow of Weatherflow for supplying observational data.

This work was supported in part by NOAA Grant NA11SEC481004 to the Cooperative Remote Sensing Science and Technology (CREST) Institute at the City College of New York, and by NOAA Regional Integrated Science Assessment (RISA) Grant NA10OAR4310212 to the Consortium for Climate Risk in the Urban Northeast (CCRUN). Some support was provided by the Department of Homeland Security under Grant Award 2008-ST-061-ML0002. The views and conclusions contained in this document are those of the authors and should not be interpreted as necessarily representing the official policies, either expressed or implied, of the Department of Homeland Security.

REFERENCES

Bornstein, R. D., 1968: Observations of the urban heat island effect in New York City. *J. Appl. Meteor.,* **7,** 575–582.

Brown, M. J., and M. Williams, 1998: An urban canopy parameterization for mesoscale meteorology models. Preprints, *Second Symp. on the Urban Environment,* Alburquerque, NM, Amer. Meteor. Soc., 144–147.

Burian, S. J., A. McKinnon, J. Hartman, and W. Han, 2005: National building statistics database: New York City. Los Alamos National Laboratory Final Rep. LA-UR-058154, 17 pp.

Chelton, D., and S. P. Xie, 2010: Coupled ocean–atmosphere interaction at oceanic mesoscales. *Oceanography,* **23** (4), 52–69.

Chen, F., and J. Dudhia, 2001: Coupling an advanced land surface–hydrology model with the Penn State–NCAR MM5 Modeling system. Part II: Preliminary model validation. *Mon. Wea. Rev.,* **129,** 587–604.

Chin, H.-N. S., M. J. Leach, G. A. Sugiyama, J. M. Leone Jr., H. Walker, J. S. Nasstrom, and M. J. Brown, 2005: Evaluation of an urban canopy parameterization in a mesoscale model using VTMX and URBAN 200 data. *Mon. Wea. Rev.,* **133,** 2043–2068.

Cohan, D. S., Y. Hu, and A. G. Russell, 2006: Dependence of ozone sensitivity analysis on grid resolution. *Atmos. Environ.,* **40,** 126–135.

Cummings, J. A., 2005: Operational multivariate ocean data assimilation. *Quart. J. Roy. Meteor. Soc.,* **131,** 3583–3604.

Ek, M., K. Mitchell, Y. Lin, E. Rogers, P. Grunmann, V. Koren, G. Gayno, and J. Tarpley, 2003: Implementation of Noah land surface model advances in the National Centers for Environmental Prediction operational mesoscale Eta Model. *J. Geophys. Res.,* **108,** 8851, doi:10.1029/2002JD003296.

Gedzelman, S. D., S. Austin, R. Cermak, N. Stefano, S. Patridge, S. Quesenberry, and D. A. Robinson, 2003: Mesoscale aspects of the urban heat island around New York City. *Theor. Appl. Climatol.,* **75,** 29–42, doi:10.1007/s00704-002-0724-2.

Grossman-Clarke, S., J. A. Zehnder, T. Loridan, and C. S. B. Grimmond, 2010: Contribution of land use changes to near-surface air temperatures during recent summer extreme heat events in the Phoenix metropolitan area. *J. Appl. Meteor. Climatol.,* **49,** 1649–1664.

Hodur, R. M., 1997: The Naval Research Laboratory's Coupled Ocean/Atmosphere Mesoscale Prediction System (COAMPS). *Mon. Wea. Rev.,* **125,** 1414–1430.

Holt, T., and J. Pullen, 2007: Urban canopy modeling of the New York City metropolitan area: A comparison and validation of single- and multilayer parameterizations. *Mon. Wea. Rev.,* **135,** 1906–1930.

Janjić, Z. I., J. P. Gerrity Jr., and S. Nickovic, 2001: An alternative approach to nonhydrostatic modeling. *Mon. Wea. Rev.,* **129,** 1164–1178.

——, T. Black, M. Pyle, E. Rogers, H. Y. Chuang, and G. DiMego, 2005: High resolution applications of the WRF NMM. *Proc. 21st Conf. on Weather Analysis and Forecasting/17th Conf. on Numerical Weather Prediction,* Washington, DC, Amer. Meteor. Soc., 16A.4. [Available online at https://ams.confex.com/ams/pdfpapers/93724.pdf.]

Jimenez, P., J. Lelieveld, and J. M. Baldasano, 2006: Multiscale modeling of air pollutants dynamics in the northwestern Mediterranean basin during a typical summertime episode. *J. Geophys. Res.,* **111,** D18306, doi:10.1029/2005JD006516.

Liu, Y., F. Chen, T. Warner, and J. Basara, 2006: Verification of a mesoscale data-assimilation and forecasting system for the Oklahoma City area during the Joint Urban 2003 field project. *J. Appl. Meteor. Climatol,* **45,** 912–929.

Loughner, C., D. Allen, K. Pickering, D. Zhang, Y. Shou, and R. Dickerson, 2011: Impact of fair-weather cumulus clouds and the Chesapeake Bay breeze on pollutant transport and transformation. *Atmos. Environ.,* **45,** 4060–4072.

Mass, C. F., D. Ovens, K. Westrick, and B. A. Colle, 2002: Does increasing horizontal resolution produce more skillful forecasts? *Bull. Amer. Meteor. Soc.,* **83,** 407–430.

Miller, S. T. K., B. D. Keim, R. W. Talbot, and H. Mao, 2003: Sea breeze: Structure, forecasting, and impacts. *Rev. Geophys.,* **41,** 1011, doi:10.1029/2003RG000124.

National Academy of Sciences, 2012: *Disaster Resilience: A National Imperative.* The National Academies Press, 244 pp.

National Research Council, 2012: *Urban Meteorology: Forecasting, Monitoring, and Meeting Users' Needs*. The National Academies Press, 176 pp.

Novak, D., and B. A. Colle, 2006: Observations of multiple sea-breeze boundaries during an unseasonably warm day in metropolitan New York City. *Bull. Amer. Meteor. Soc.,* **87,** 169–174.

Oke, T. R., 2006: Initial guidance to obtain representative meteorological observations at urban sites. Instruments and Observing Methods Rep. 81, WMO/TD-1250, 47 pp.

Orton, P. M., W. R. McGillis, and C. J. Zappa, 2010: Sea breeze forcing of estuary turbulence and CO_2 exchange. *Geophys. Res. Lett.,* **37,** L13603, doi:10.1029/2010GL043159.

Pullen, J., T. Holt, A. Blumberg, and R. Bornstein, 2007: Atmospheric response to local upwelling in the vicinity of New York–New Jersey harbor. *J. Appl. Meteor. Climatol,* **46,** 1031–1052.

Rosenfeld, A. H., and Coauthors, 1995: Mitigation of urban heat island: Materials, utility, programs, updates. *Energy Build.,* **22,** 255–265.

Rosenzweig, C., and Coauthors, 2009: Mitigating New York City's heat island: Integrating stakeholder perspectives and scientific evaluation. *Bull. Amer. Meteor. Soc.,* **90,** 1297–1311.

Sailor, D., 2011: A review of methods for estimating anthropogenic heat and moisture emissions in the urban environment. *Int. J. Climatol.,* **31,** 189–199, doi:10.1002/joc.2106.

Tan, J., and Coauthors, 2009: The urban heat island and its impact on heat waves and human health in Shanghai. *Int. J. Biometeor.,* **54,** 75–84.

Thompson, W., T. Holt, and J. Pullen, 2007: Investigation of a sea breeze front in an urban environment. *Quart. J. Roy. Meteor. Soc.,* **133,** 579–594.

Zhong, S., and E. S. Takle, 1992: An observational study of sea-and-land breeze circulation in an area of complex coastal heating. *J. Appl. Meteor.,* **31,** 1426–1438.